

## Chapter

# Long-Term Monitoring of Slope Movements with Time-Domain Reflectometry Technology in Landslide Areas, Taiwan

*Miau-Bin Su, I-Hui Chen, Shei-Chen Ho, Yu-Shu Lin  
and Jun-Yang Chen*

## Abstract

The study employs time-domain reflectometry (TDR) technology for landslide monitoring to explore rock deformation mechanism and to estimate locations of potential sliding surfaces in several landslide areas, Taiwan, over ten years. Comparing to laboratory and field testing, sliding surfaces in landslide areas occurred mainly at two types, namely shear and extension failure. The TDR technology is used for field monitoring to analyze locations of sliding surfaces and to quantify the magnitude of the sliding through laboratory shear and extension tests. There are several TDR-monitoring stations in six alpine landslide areas in the middle of Taiwan for long-term monitoring. A relation between TDR reflection coefficients and shear displacements was employed for a localized shear deformation in the field. Furthermore, the type of a cable rupture for the TDR monitoring in landslides can be determined as shear, extension, or compound failure through the field TDR waveforms. Overall, the TDR technology is practically used for a long-term monitoring system to detect the location and magnitude of slope movement in landslide areas.

**Keywords:** time domain reflectometry (TDR), landslide monitoring, slope movement, shear and extension testing, deformation quantification

## 1. Introduction

Determining the location and magnitude of sliding surfaces is a vital measure for landslide monitoring. For conventional slope monitoring, drill-log reports can illustrate in situ presence of weak rock or location of weak rock masses [1, 2]. Furthermore, inclinometers are used for landslide monitoring to detect sliding zones and to measure the subsurface lateral displacement of soil or rock [3–5]. However, it is time-consuming and difficult by these traditional methods to interpret an accurate location of sliding surface in a landslide area [6, 7]. In recent years, time-domain reflectometry (TDR) is employed for the monitoring of slope movement to locate depths of slope failures [8, 9]. The TDR technology uses a cable tester to detect a coaxial cable grouted in a borehole. While the cable broken or ruptured, a TDR signal

from the cable tester is reflected. The reflection shows the location of sliding surfaces and the effect of TDR-cable length can be determined accurately [10–13].

There are some characteristics of the TDR technology for the monitoring of landslide deformation. Firstly, a coaxial cable is a continuous sensor where the TDR system can interrogate reflection coefficients of a crimp, kink, extension, or break [14]. Secondly, an important ability for the TDR technology is to locate the relative movement along the cable by extended or shear stress that causes the change of cable characteristic impedance when two adjacent rock masses move each other [15, 16]. Finally, reflection coefficients of TDR-cable deformation are positive correlations with the rate of slope movement [9, 17, 18].

There are two main themes in this research. The first is for laboratory experiments that include shear and extension tests with grouted cables. The TDR technology can interrogate reflected waveforms corresponding to the cable deformation in order to get a relation between reflection coefficients and the magnitude of cable deformation [17]. The other theme is for field TRD monitoring. There are several TDR monitoring stations in six landslide areas where occurred some slides in Taiwan [6, 17–19]. Finally, the study analyzes field data from TDR monitoring stations to compare to results of quantification in laboratory tests and to determine the location, type, and magnitude of slope movement for long-term monitoring in the landslide areas.

## **2. Laboratory testing for TDR technology**

For literature reviews of TDR laboratory experiments, a TDR tester detected reflection coefficients of a grouted coaxial cable when the cable is deformed by shear or extension stress as shown in **Figure 1(a)**, which illustrated a signal “spike” as like a shape of “V” by shear stress (**Figure 1(b)**) and another signal as like a shape of “concave” by extension stress (**Figure 1(c)**) based on the TDR theories [15, 16].

Whether shearing deformations are big or small, the magnitude of TDR reflected waveforms is significant correlation with cable deformation [20, 21]. An integrated area method is proposed to quantify the magnitude of a TDR reflected waveform on the deformation of rock masses and concrete structures through laboratory bench tests [10, 17]. The method involved the integration of the TDR voltage signal over time in **Figure 2**, which means that L1 is the start point of a TDR reflected waveform due to a change in capacitance and L2 is an end point when the voltage returns to its reference level [17].

For laboratory tests, each coaxial cable was grouted into a cement test specimen, which was 1-m in length and 10 cm in diameter. Then, each test specimen was installed on a bench, as shown in **Figures 3** and **4**, which were twofold. One is to determine a relation between the magnitude of cable deformations and TDR reflected waveforms by shear displacement. The second is to measure a change length of the cable with TDR reflected waveforms by extension displacement.

The laboratory testing was designed to define a relation between the TDR reflection coefficients and the magnitude of cable deformation by shear and extension failure. For example, a coaxial cable was grouted into a cement test specimen with 1 m in length and then connected to a TDR cable tester (HL 1101). The test specimen was installed on a bench, which was divided into three 20-cm-length and 10-cm-diameter units, named S1, S2, and S3, as shown in **Figure 3**. Then, a TDR tester (HL1101) sent a voltage pulse waveform that travels along a coaxial cable. Finally, data from the tester were transmitted to a PC and was displayed as TDR waveforms. The cable and grout were the same as the materials used in field installation, listed in **Table 1** [17].

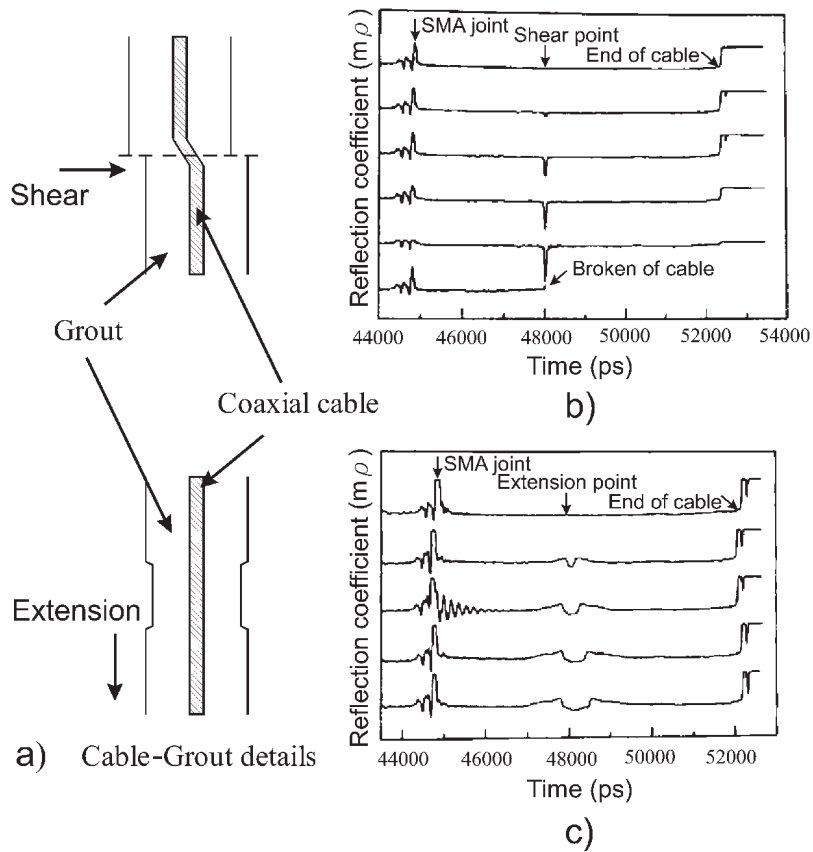


**Figure 1.** Diagrams of reflected waveforms of TDR coaxial cables in grout by shear and extension movement. (a) grouted cables deformed by shear or extension stress; (b) changes in reflection coefficients of TDR waveforms for shear tests; (c) changes in reflection coefficients of TDR waveforms for extension tests [15, 16].

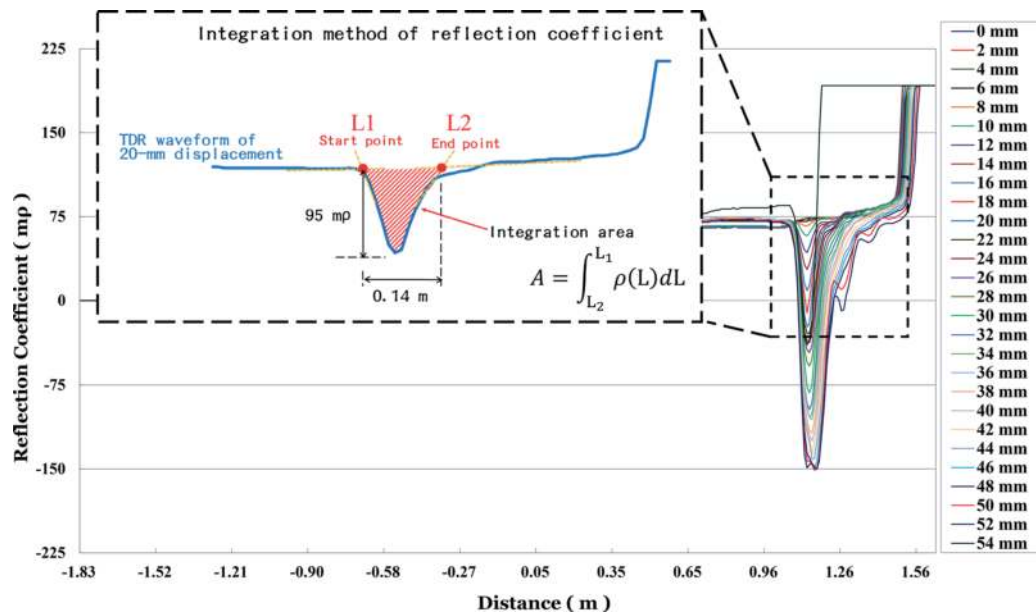


**Figure 2.** Integration method of the TDR waveform for shear displacement [17].

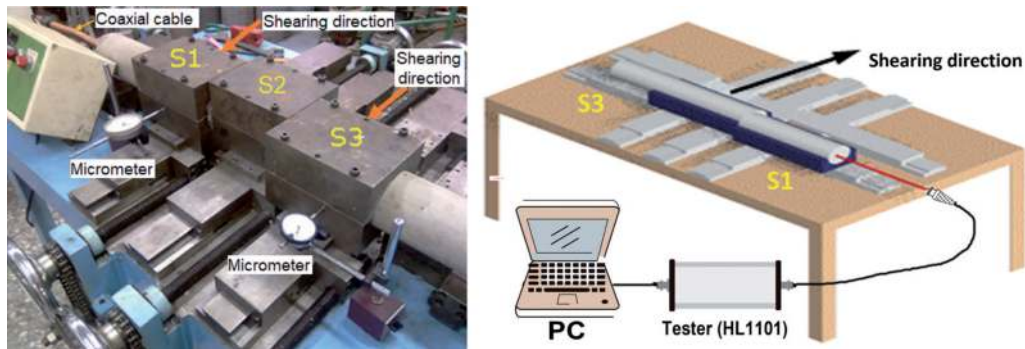


**Figure 3.** Instrumentation of shear bench test (adapted from [17]).



**Figure 4.** Instrumentation of extension bench test (adapted from [18]).

Coaxial cable Type	Diameter (mm)	Grout cement Type	Grout mix ratio (water to cement)	Compressive strength (kgf/cm <sup>2</sup> )
CTLLCX 7/8" CFC	Φ25 mm	Portland cement I	1:3	146.5

**Table 1.** Properties of the TDR cable and grout [17].

For the shear test, S1 and S3 were shear units, but S2 was a fixed unit in **Figure 3**. The S1 was set at a given shear displacement of 0, 10, 20, 30, and 40 mm, and then the S3 was sheared successively at 2-mm intervals for each shear displacement of the S1, respectively, until the cable rupture [17]. Results of the TDR interrogated waveforms for the cable were plotted in **Figure 5(a)** where the TDR signals (reflection coefficient in millirhos) represented the amplitude of reflected waveforms at a distance in meter along the cable [17]. As can be seen in **Figure 5(b)**, the shear displacement at the S3 location is 52 mm before the cable rupture corresponding to the reflection coefficient at 233 mp.

All shear tests have the same tendencies as the graph of **Figure 5** for the TDR responses of the S1 and S3 displacement, so there existed a significant relation between shear displacements and reflection coefficients, as shown in **Figure 6**, which illustrated the maximum and average magnitude of the cable deformation by shear failure that were 60 and 47 mm, respectively [17]. A linear relationship between shear deformation and TDR reflection magnitude is attractive due to its simplicity, which has been used extensively to quantify the magnitude of shear deformation [8]. Finally, the study uses the linear regression to determine the

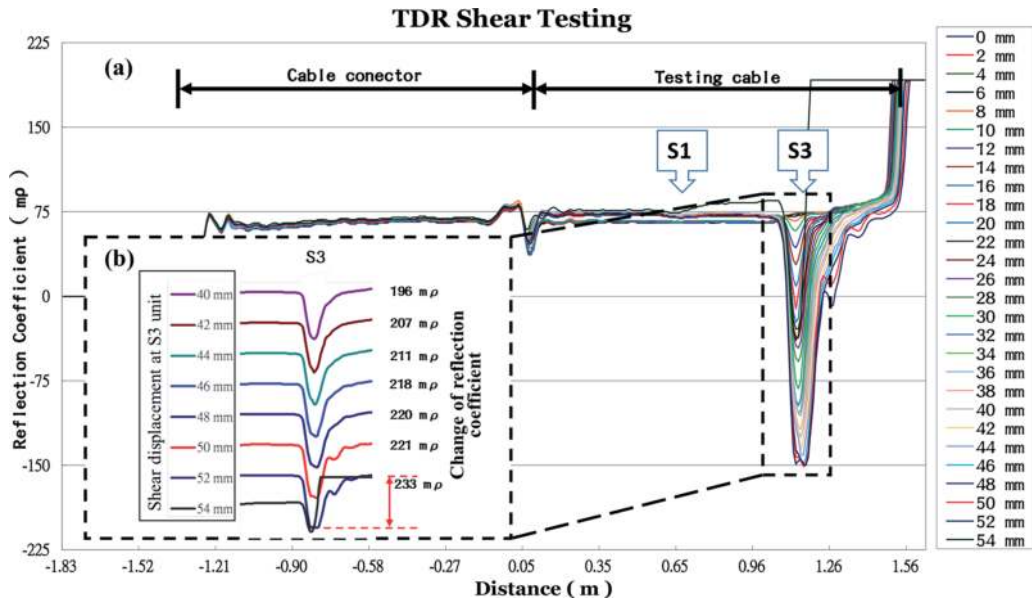


**Figure 5.** Graph of reflected waveform changes at S3 shear plane as S1 shear displacement is set at 0 mm. (a) changes in reflection coefficients of TDR waveforms for the whole grouted cable; (b) enlarged graph of changes in reflection coefficients of TDR waveforms at S3 shear plane [17].

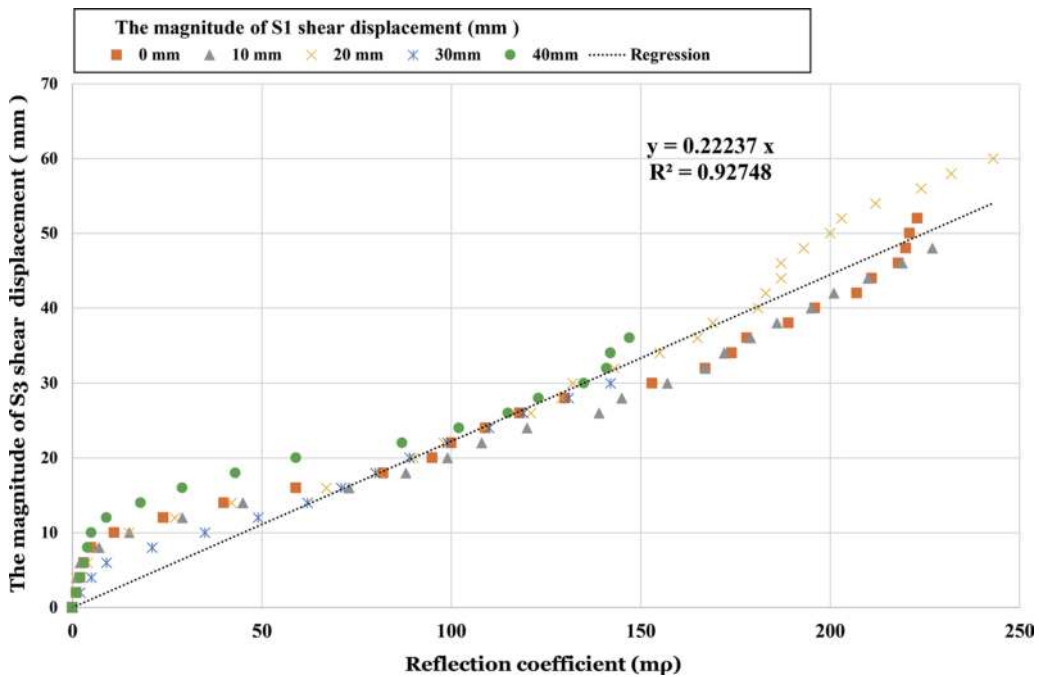


**Figure 6.** Graph of the relationship between the shear displacement (millimeters) and reflection coefficient (mρ) in shear tests [17, 18].

magnitude of shear deformations in the field corresponding to relative changes of reflection coefficients interrogated by on-site TDR system [17, 18].

For the extension test, a 1-m test specimen was installed on the bench, which was set as two 20-cm-length units; one was a moving unit T1 and the other was fixed, as shown in **Figure 4** [18]. The amount of extension displacement at the T1 location successively incremented at 5 mm until the cable ruptured and results



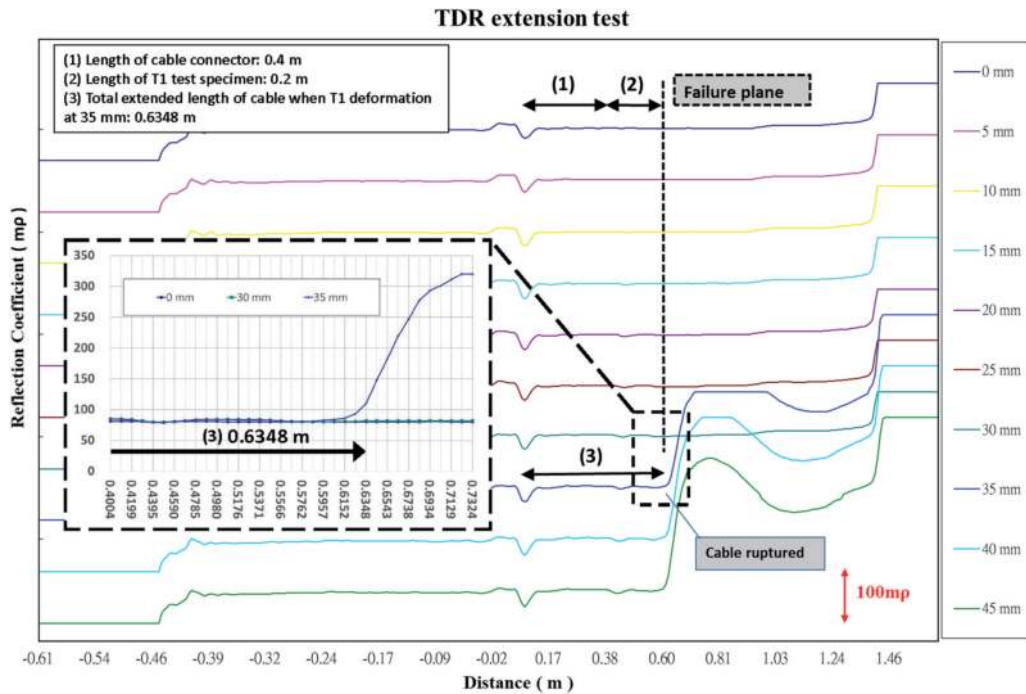


**Figure 7.**  
 Graph of reflected waveform changes in extension tests [18].

of the extension test was plotted in **Figure 7**, which shows that the magnitude of extension displacement is 35 mm as the cable rupture [18]. A change in length of the cable between first waveform and the 35-mm-test waveform was measured to 0.0348 m that was almost the same as the magnitude of extension displacement at 35 mm. Thus, the result can be employed to measure the magnitude of extended cable in field TDR monitoring [6, 18].

### 3. Principle of the TDR monitoring in landslide areas

A diagram of on-site TDR instrumentation is shown in **Figure 8**. A coaxial cable is grouted with cement into a borehole in a slope. A TDR cable tester (HL1101) sends and receives a voltage pulse waveform that travels along the coaxial cable through a connector. A transmission of the TDR signal through the tester is stored in a microcomputer that is an embedded system after the signal is reflected by a cable deformation.

There are six TDR-monitoring stations in different landslide areas, Taiwan, including Lishan, Song-Mao, Old Tribe, and New Jia-Yang areas since 2008, and Jiufenershan and Lushan areas since 2012 and 2018, respectively. For the first four areas, the distribution of TDR-monitoring stations was shown in **Figure 9**, which illustrated representative stations called B5, L2, J1, and S9 monitoring stations in the four areas. The four landslide areas are located at the middle of Taiwan with altitude between 1800 and 2100 m, inclination toward the northwest and slope angle of 15–30° [22]. Geologically, the areas belong to colluvium and slate formation. In April 1990, a severe landslide occurred in Lishan area after prolonged torrential rainfall. After that, governments remedied the area with many drainage works and slope monitoring systems in order to prevent from disasters again [6].

The TDR cable of 40–50 m in depth was grouted into a borehole every station. All TDR waveforms of different date are recorded every month so that it is easy

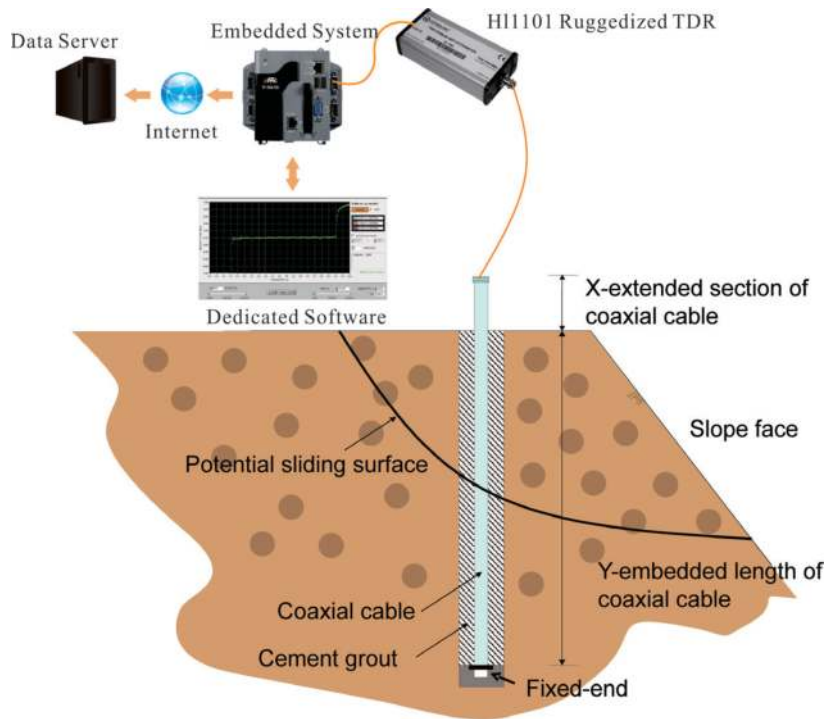


**Figure 8.**  
*Diagram of on-site instrumentation for the TDR technology (adapted from [18]).*

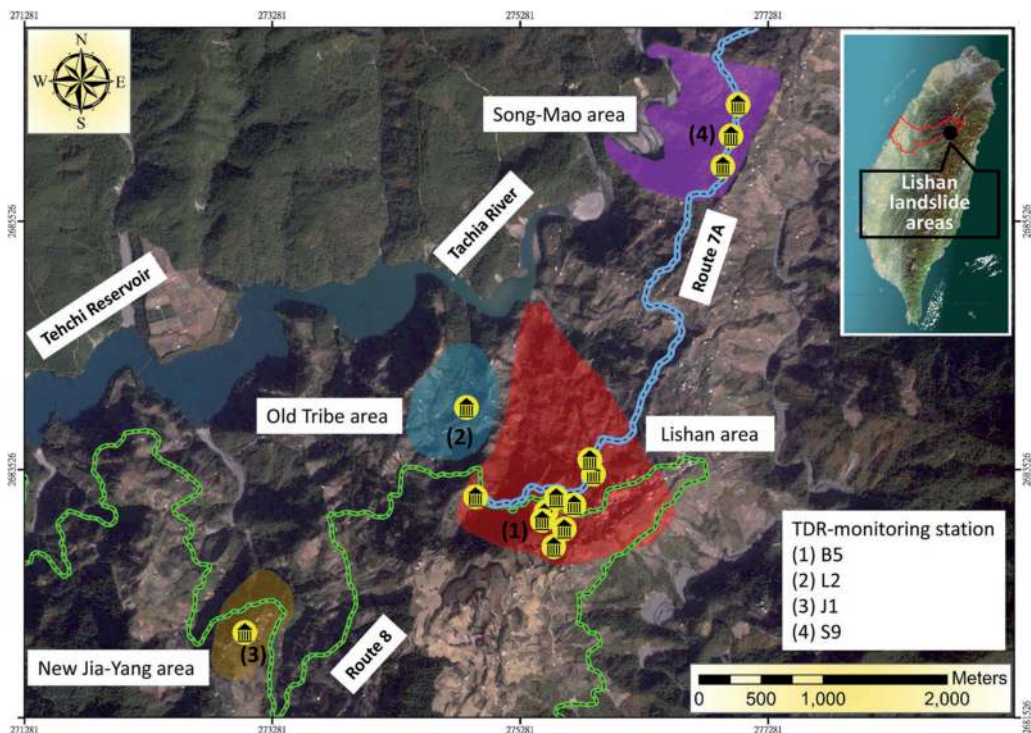


**Figure 9.**  
*Location map of TDR monitoring stations in four landslide areas.*

to interpret a change of waveforms at any depth where a slope movement could occur. For example, records of the TDR monitoring at J1 TDR-monitoring station in New Jia-Yang landslide area were plotted in **Figure 10**. They revealed changes in

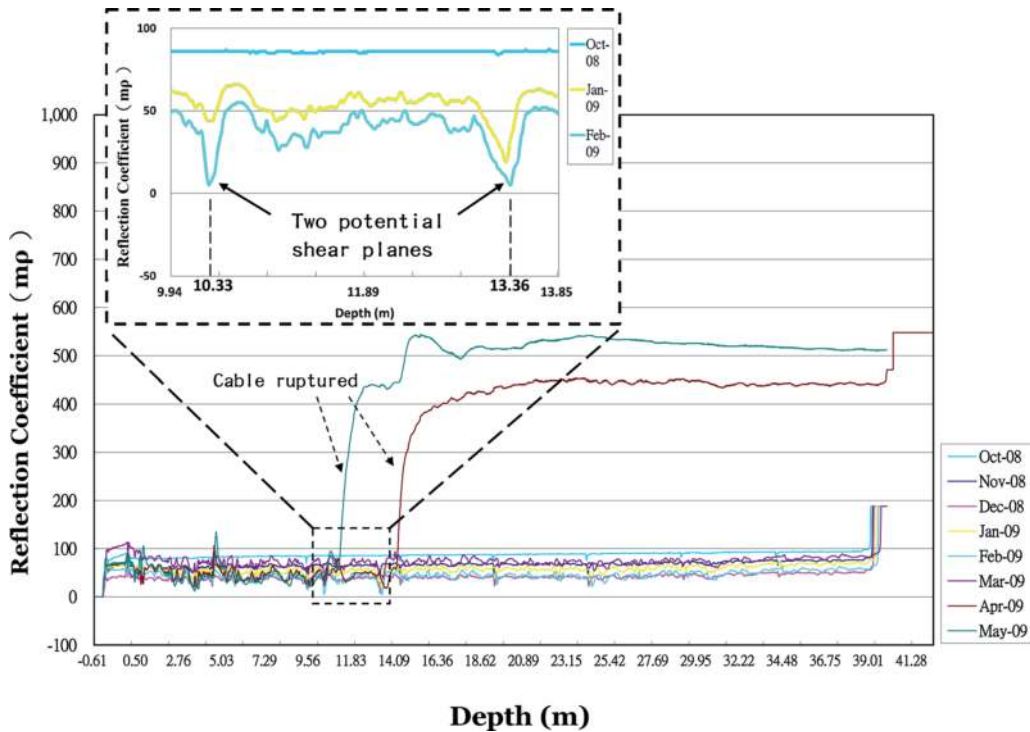


**Figure 10.**  
Recorded waveform at J1 TDR-monitoring station [17].

reflection coefficients at the J1 station since 2008. The changes in TDR waveforms from 10/2008 to 05/2009 shown in the enlarged graph of **Figure 10** were caused by two spikes at 10.33 and 13.36 m in depth at the station, respectively [17]. Thus, significant increases of amplitudes in the reflection coefficient occurred at the two depths in April and May 2009, indicating that the cable was ruptured at two locations by shear failure [6, 17].

The other case study is in Jiufenershan landslide area that is located at the middle of in Taiwan, as shown in **Figure 11**. The area occurred due to a severe landslide triggered as a result of the 1999 earthquake. The geology of the landslide area with altitude between 500 and 2100 m is underlain mainly by Miocene sedimentary and shale formations where the strike is N36°E and the dip is 21°SE [23]. Since 2003, there has been a landslide monitoring project for the Jiufenershan landslide with some monitoring equipment, including extensometers, inclinometers, groundwater level gauges, etc. The TDR technology was installed in the area since 2012 in order to monitor slope movement in the area [18].

From the 12/2012 and 01/2013 TDR records in Jiufenershan landslide area (**Figure 12**), there were significant deformations at 7.51- and 35.72-m depths at N2 station because there existed localized cable ruptures [18]. Based on the regression of the relation between cable deformation and reflection coefficient in the laboratory, 47-mm displacement of the cable corresponds to approximately the TDR reflection coefficient of 210 mp that can be regarded as the working limit for the cable rupture by deformed failure in the case study [18].

For the last case study in Lushan landslide area, it is located in central Taiwan with an altitude from 1050 to 1480 m, as shown in **Figure 13** [19]. The bedrock of the slope mass is mainly composed of slate with strikes of cleavage range from N10° to 40°E. The slope is defined as composed of 20-m-thick colluvium near the



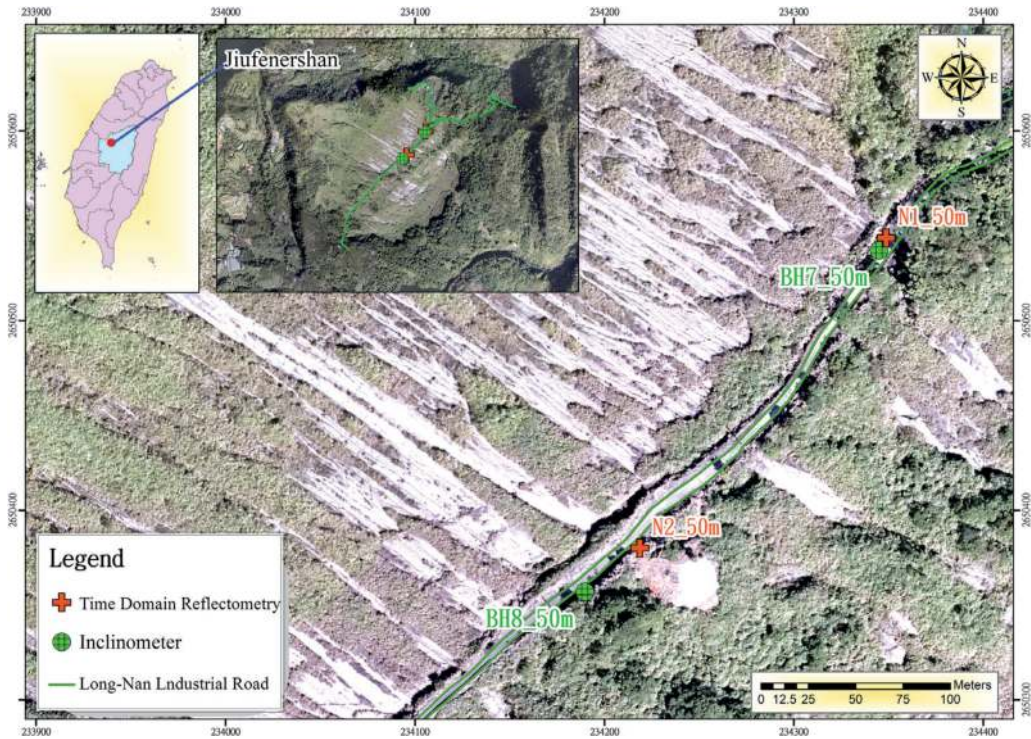


**Figure 11.**  
 Location map of the monitoring stations in Jiufenershan landslide area [18].

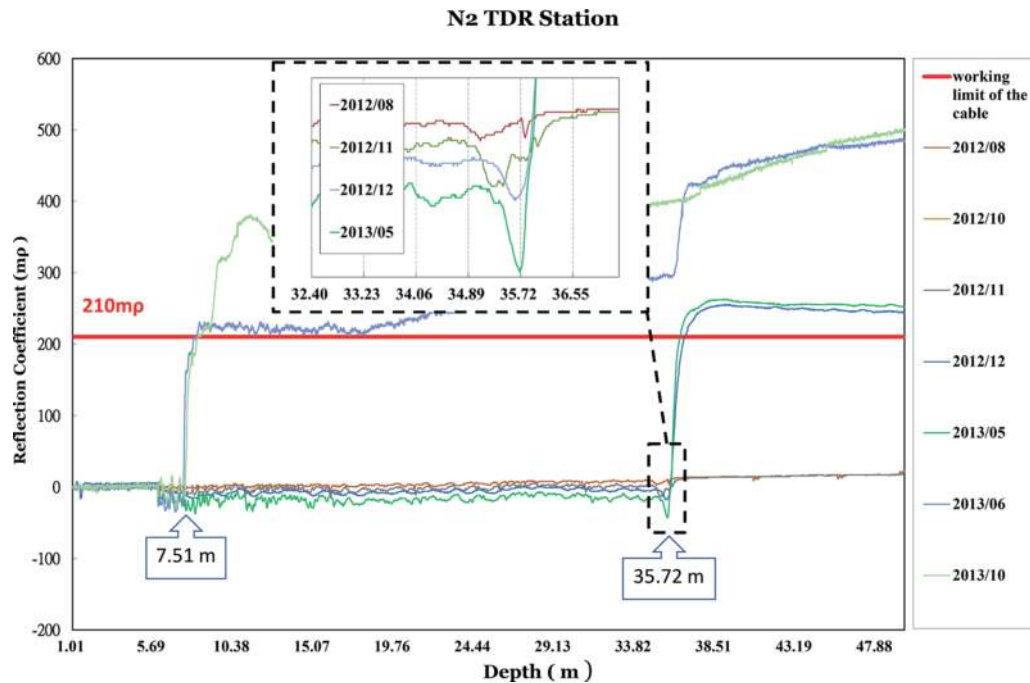


**Figure 12.**  
 Changes of reflection coefficients interrogated by the TDR at N2 monitoring station [18].

surface and fresh slate at bottom [24]. The Lushan formation in the area belongs to the attitude of the foliation, which influences the mass rock creep structures of foliated rocks and may experience deformation by potential landslides [25]. There

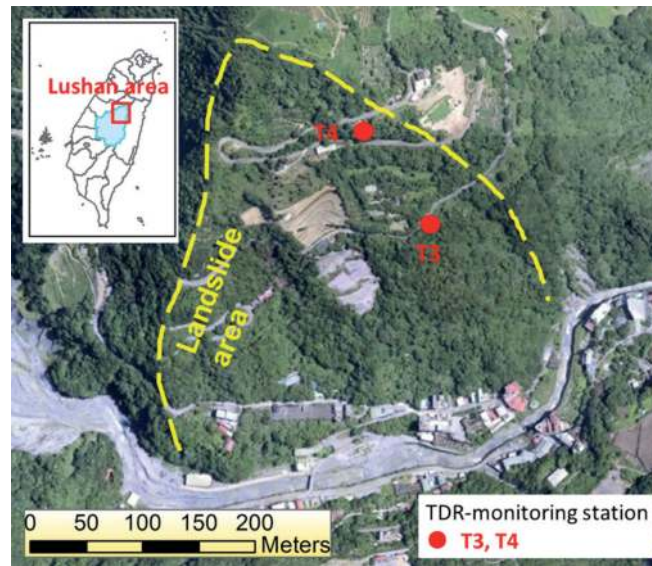


**Figure 13.**  
Location and geologic map in Lushan landslide area.

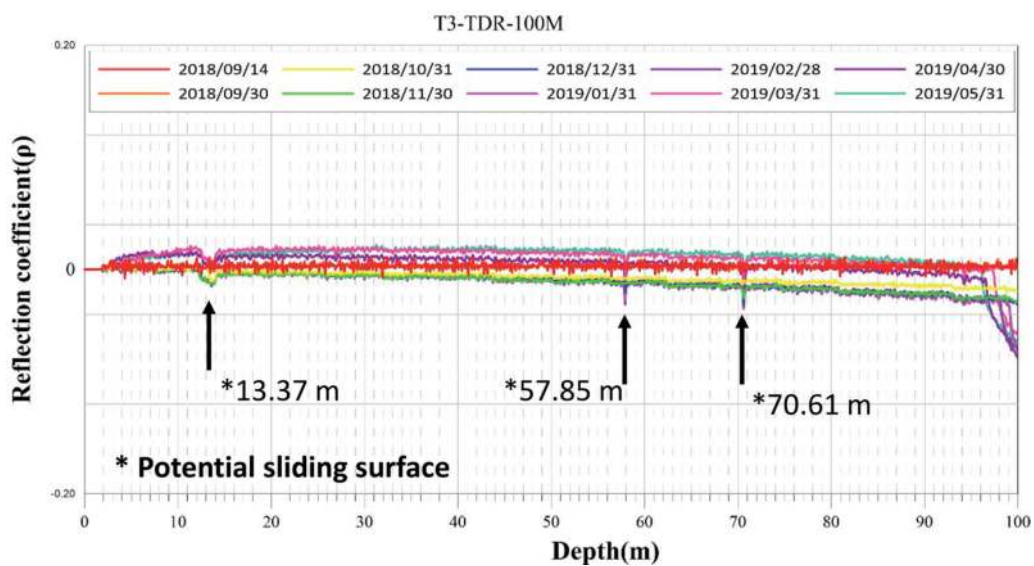


**Figure 14.**  
Records of TDR reflected waveforms at T3 monitoring station (adapted from [19]).

are two TDR-monitoring stations, coded T3 and T4, in the area where coaxial cables of approximately 100-m length were grouted with cement to monitor potential slope movement.

For example, records of T3 TDR-monitoring waveforms from Sep 2018 to May 2019 were plotted in **Figure 14**. Changes in TDR waveforms were caused by three spikes at approximately 13, 57, and 70 m in depth at the T3 station [19]. These TDR signals “spikes” can be indicated as the location of localized shear failure through the laboratory testing in the study. Furthermore, significant increases in amplitudes in the reflection coefficient occurred at the three depths from September 2018 to May 2019, indicating that the cable was partially broken at the three locations by shear deformation at T3 [19].

#### 4. Results and discussions of field monitoring

According to the result of laboratory tests and the data from field monitoring, the type and magnitude of slope movement in the landslide areas can be determined. All recorded waveforms of different dates were separately plotted in a graph to easily compare changes in waveforms of the TDR monitoring. Thus, records of the TDR waveforms in the landslide areas were replotted in **Figures 15–18** that showed changes in reflection coefficients of the four stations (B5 in Lishan area, J1 in New Jia-Yang area, L2 in Old Tribe area, and S9 in Song-Mao area). TDR-cable signals presented the amplitude of reflected waveforms at a given distance corresponding to the depth of a grouted cable at TDR-monitoring stations. Then, the waveforms can be easily interpreted by a change of waveforms at a depth where shear failure occurred or at an extended length of the grouted cable where extension failure occurred.

As illustrated in **Figure 15**, no significant change in the waveforms occurred at the B5 station from 2016 to 2018 because remedial works had been performed to prevent the area from additional sliding. Alternatively, some TDR waveforms changed at the other three stations from 2008 to 2015 in **Figures 16–18**, which illustrated that the type of waveform changes was shear displacement and extension signals.

For J1 TDR-monitoring station, the TDR waveforms were formed as like the shape of “V” at a depth of approximately 13 m in **Figure 16**, which illustrated the type of the waveform by shear stress [17]. Based on the laboratory tests, the magnitude of the shear displacement in **Figure 16** was more than 47 mm in July 2009 because the reflection coefficient in the spike of the TDR waveform was over 210 mp that means the localized cable ruptured.

From another point of view in other graphs, some TDR waveforms of other areas were formed as the type of extension failure such as L2 and S9 stations because the type of the waveforms was similar to the type of the laboratory extension testing and total length of the two cables was extended at the end of them. As shown by the Mar/2009 TDR record in **Figure 17**, there was an extended displacement at a

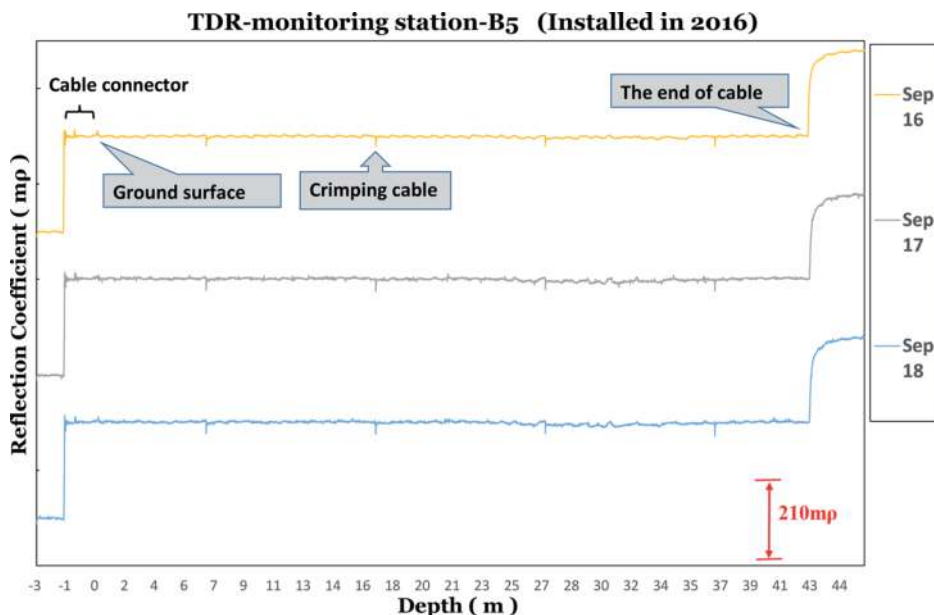


**Figure 15.**  
*Graph of TDR reflected waveforms at B5 TDR-monitoring station.*



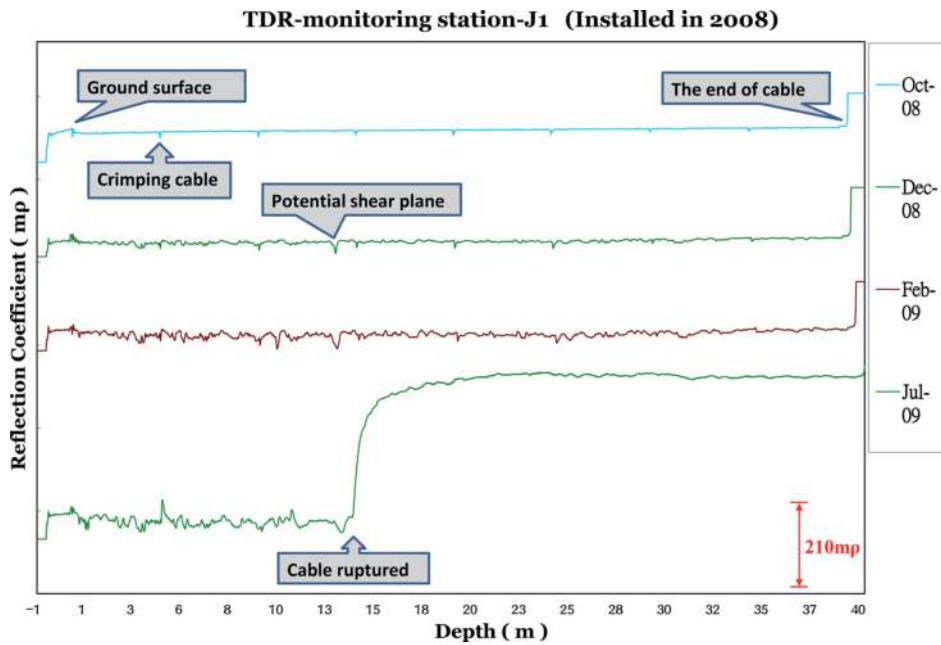


Figure 16. Graph of TDR reflected at J1 TDR-monitoring station.

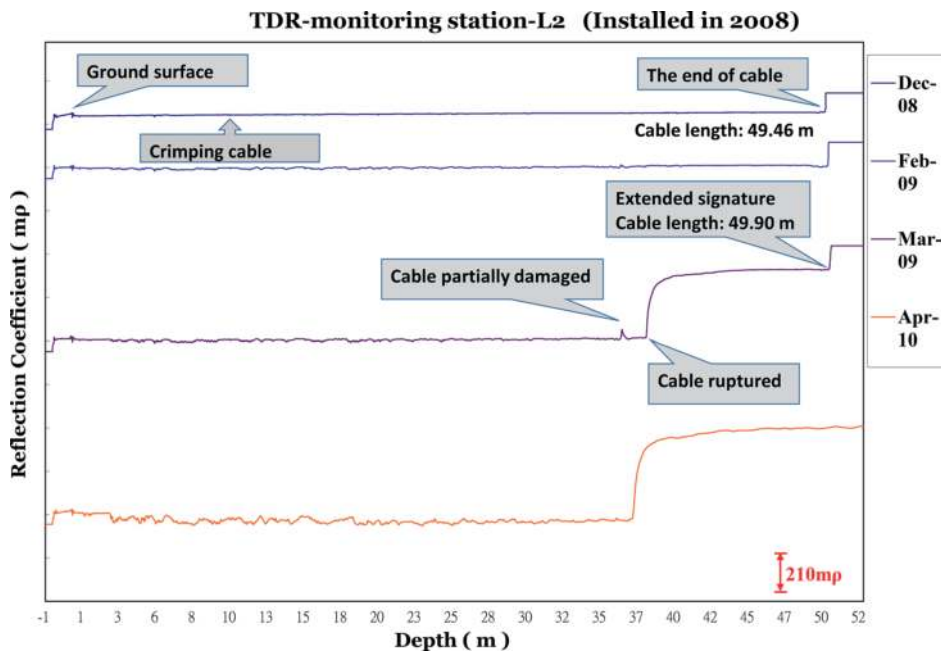
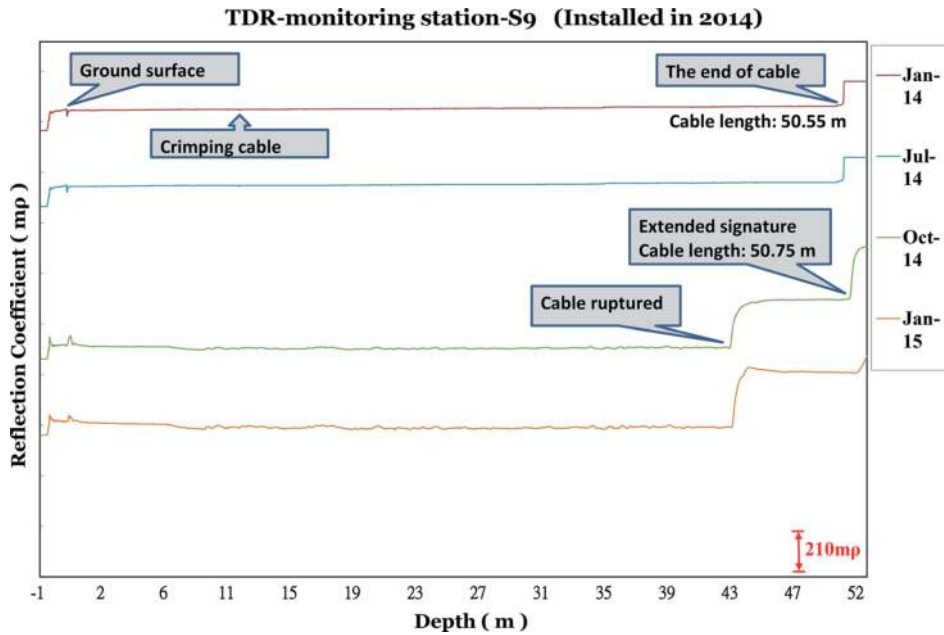


Figure 17. Graph of TDR reflected at L2 TDR-monitoring station.

depth of 37.87 m at L2 station when the waveform signal showed the cable ruptured. As can be seen from **Figure 18**, the cable was extended to a depth of 43.23 m at S9 station in October 2014. Also, there were considerably extended lengths of the end cables at L2 and S9 stations, by 0.44 and 0.20 m, respectively.

For N2 TDR-monitoring station in Jiufenershan landslide area, records of on-site TDR monitoring waveforms were replotted in **Figure 19** that showed the TDR waveforms were formed as signals of cable rupture at 7.51- and 35.72-m depth marked as A and B, respectively [18]. As shown by the 11/2012 TDR record of the enlarged





**Figure 18.**  
 Graph of TDR reflected at S9 TDR-monitoring station.

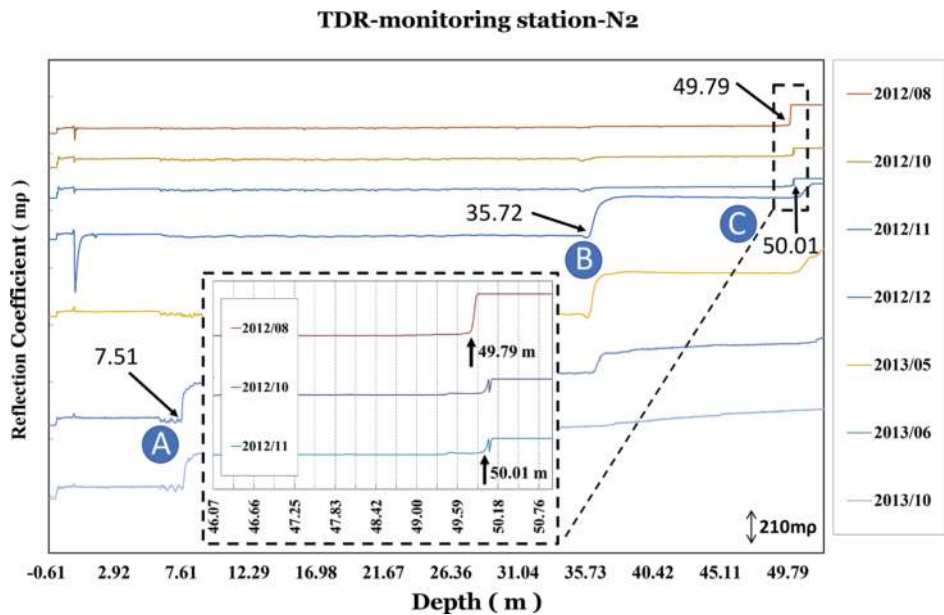


**Figure 19.**  
 Graph of TDR reflected at N2 TDR-monitoring station [18].

chart in **Figure 19** (mark C), the total length of the cable had been extended by potential extension stress from 49.79 to 50.01 m measured by the TDR signal at the end of the cable. It was obvious that the cable was deformed by extension stress initially [18]. However, for the enlarged graph in **Figure 12**, there was a pulse-like signal of the waveform at a 35.72-m depth in November 2012 that was similar to a spike type generated by laboratory shear testing; thus, the cable was deformed by shear stress at the location before the cable rupture in December 2012, despite the fact that the cable had been extended from August 2012 to November 2012. As a result, the cable would be damaged by compound failure in the landslide area [18].

For T3 TDR-monitoring station in Lushan landslide area, original records of TDR-monitoring waveforms were replotted as a graph rotated vertically so that it is easy to observe changes of TDR waveforms in vertical depth under the ground at the T3 station, as shown in **Figure 20** where  $x$  axis means the T3 shear displacement in centimeters calculated using the linear regression equation in the laboratory testing [18, 19].

There were three shear surfaces at approximately 13-, 57- and 70-m depths in **Figure 20** as well as in **Figure 14**. Through the laboratory testing, the magnitude of cable sheared deformation can be determined for the field slope movement corresponding to the TDR reflection coefficients in the T3 TDR monitoring. For example, increases in the amplitudes of reflection coefficients occurred at two spikes at approximately 57- and 70 m depths from September 2018 to May 2019 in the enlarged graph of **Figure 20**. The magnitude of the cable sheared deformation at the two depths was calculated using the linear regression equation  $y = 0.22247x$  (see **Figure 6**, where  $y$  means shear displacement in millimeters and  $x$  means a change of reflection coefficients in  $\rho$ ; [18, 19]). Then, the changes in reflection coefficients of the two localized shear locations were detected as 0.03 and 0.024  $\rho$  (30 and 24  $\mu\rho$ ) corresponding to shear displacement by 6.7 and 5.6 mm, respectively, on May 31, 2019. It was obvious that these TDR signal “spikes” can be indicated as the type of localized shear failure through the laboratory testing in the study. Meanwhile,

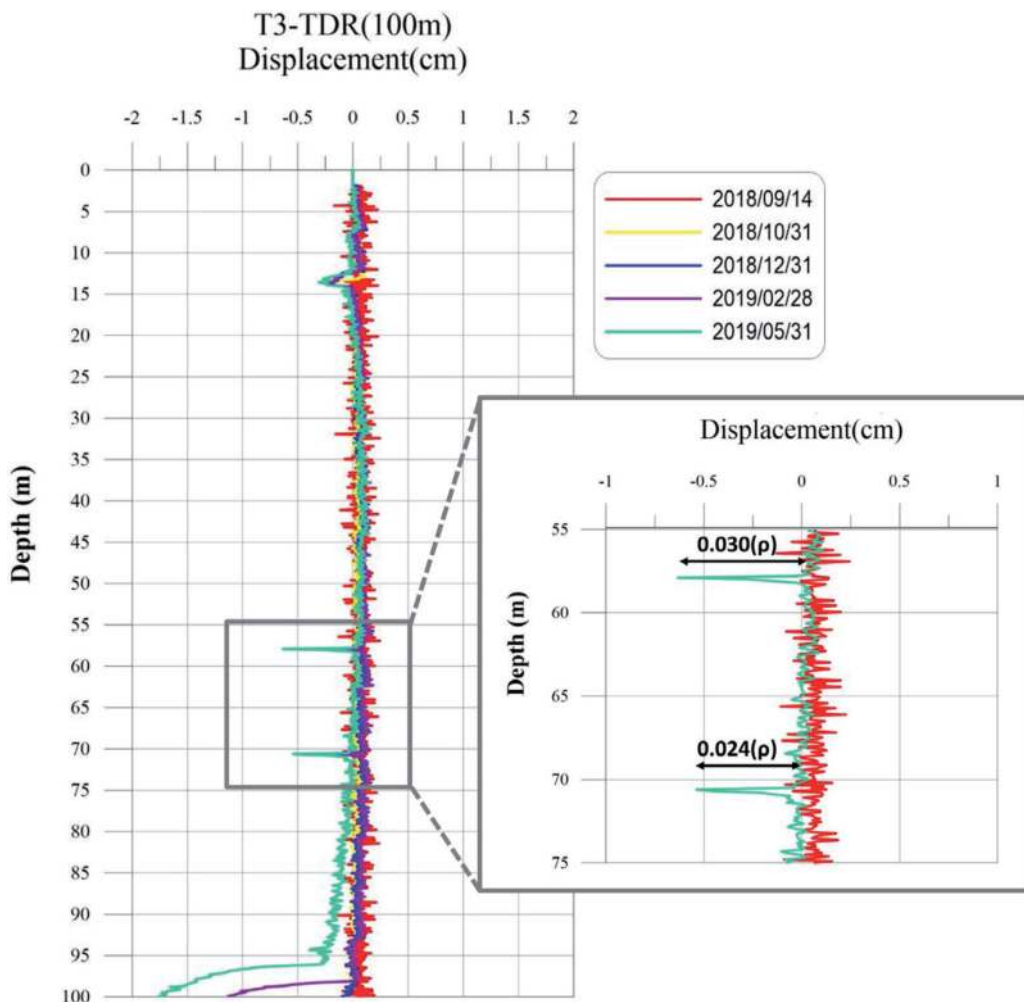


**Figure 20.**  
Graph of TDR reflected waveforms at T3 TDR-monitoring station.

Area	Monitoring station	Time	Failure depth (m)	Failure type	Magnitude (m)
Lishan	B5	September 2015 to September 2017		No significant deformation	
New Jia-Yang	J1	May 2009	10.33	Shear	More than 0.047
		April 2009	13.36	Shear	More than 0.047
Old Tribe	L2	March 2009	37.87	Extension	Extended length: 0.44
Song-Mao	S9	October 2014	43.23	Extension	Extended length: 0.20
Jiufenershan	N2	December 2012	35.72	Coexistence of extension and shear type	Extended length: 0.22
		June 2013	7.51		
Lushan	T3	May 2019	13.37	Shear	0.0069
		May 2019	57.85	Shear	0.0067
		May 2019	70.61	Shear	0.0056

**Table 2.**  
 Location and magnitude of shear deformation in landslide areas, Taiwan.

reflection coefficients of the T3 TDR monitoring did not reach 210 mρ so the cable did not rupture. However, significant increases of amplitudes in the reflection coefficient occurred at three depths from September 2018 to May 2019 so that the area could consecutively occur as mass rock creep in Lushan landslide area [19].

By the method of the linear regression calculation, all magnitude of localized shear displacements at sliding surfaces at every TDR-monitoring station in the six landslide areas can be determined, as presented in **Table 2**. On the other hand, all magnitude of extended cables at L2, S9, and N2 stations can also be measured as shown in **Table 2**. In particular, the data from the N2 station inferred that sliding deformation in the landslide area would be a compound type that means the slope movement may be a coexistence of extension-type and shear-type deformation through the result of field TDR waveforms [18]. The magnitude of extension deformation was 0.22 m from August 2012 to November 2012 at N2 station. Also, the cable of N2 had been ruptured because the reflection coefficient of the TDR waveforms had been over 210 mρ (see **Figure 12**) according to the result of the laboratory testing.

Overall, if a reflection coefficient of a TDR monitoring station reaches to 210 mρ or more in the field, it could mean that a TDR cable could be damaged by potential slope deformation through the result of the laboratory and field tests. Average 47 mm of shear displacement in a TDR cable corresponds to the TDR reflection coefficient of 210 mρ that can be defined as the working limit for the cable ruptured by shear failure in these case studies. Nevertheless, the maximum amount of cable extension can reach 22 and 44 cm in Jiufenershan and Old Tribe landslide area, respectively. Finally, the TDR technology can determine the type, location, and magnitude of slope movement in the landslide areas although field TDR waveforms were complicated and diverse. The TDR technology is practical and successful for landslide monitoring to interpret the location and magnitude of sliding surfaces in the case studies.

## 5. Conclusions

The study employed the TDR technology for the landslide monitoring of slope movement to determine the location and magnitude of sliding surfaces in six landslide areas. Comparing to laboratory and field tests, the TDR monitoring of J1 in New Jia-Yang landslide area detected two sliding surfaces at 10.33- and 13.36-m depths where the magnitude of sliding deformation was estimated at more than 47 mm, because the reflection coefficients of the TDR monitoring were over 210 m $\rho$ . For the TDR monitoring of L2 and S9, the extended length of each grouted cable can be measured by 44 and 20 cm, while the two cables had been ruptured at 37.87- and 43.23-m depth, respectively. For the TDR monitoring of J1, there were cable ruptures at depths of 7.51 and 35.72 m where rock mass slides was extension-type and shear-type compound failure. Finally, the TDR monitoring of T3 consecutively detected three sliding surfaces at 13.37-, 57.85- and 70.61-m depths where slight deformation amount was estimated by 0.31, 0.67, and 0.53 cm, respectively, using the linear regression equation of the relation between TDR reflection coefficients and shear displacements in the shear tests.

Overall, the TDR technology can accurately detect the location of TDR cable deformation for the monitoring of slope movement in the landslide areas. Meanwhile, sliding types of shear, extension, or compound failure can be determined using the change of TDR reflected waveforms in the laboratory and field. Finally, 210-m $\rho$  reflection coefficients of TDR monitoring can be a threshold of a partial cable ruptured corresponding to the cable sheared deformation of 47 mm in the case studies. In the future, the TDR technology can be an early warning system before a landslide occurs.

## Acknowledgements


The field test presented in this paper could be realized through the support and sponsorship of the Soil and Water Conservation Bureau (SWCB), Council of Agriculture, Executive Yuan, Taiwan. Consecutive projects including long-term monitoring are proposed and approved by the technical counseling committee on the remediation works of large-scale landslide areas, the SWCB. Furthermore, the performance evaluation of each project is periodically reviewed by the committee annually.

## Author details

Miau-Bin Su, I-Hui Chen\*, Shei-Chen Ho, Yu-Shu Lin and Jun-Yang Chen  
Department of Civil Engineering, National Chung Hsing University, Taichung City, Taiwan

\*Address all correspondence to: [ian.cih82@gmail.com](mailto:ian.cih82@gmail.com)

## IntechOpen

© 2019 The Author(s). Licensee IntechOpen. This chapter is distributed under the terms of the Creative Commons Attribution License (<http://creativecommons.org/licenses/by/3.0>), which permits unrestricted use, distribution, and reproduction in any medium, provided the original work is properly cited. 



## References

- [1] Goodman RE. Introduction to Rock Mechanics. 2nd ed. New York: Wiley; 1989
- [2] Blackburn JT, Dowding CH. Finite-element analysis of time domain reflectometry cable-grout-soil interaction. *Journal of Geotechnical and Geoenvironmental Engineering*. 2004;**130**(3):231-239
- [3] Dowding CH, Su MB, O'Connor KM. Measurement of rock mass deformation with grouted coaxial antenna cables. *Rock Mechanics and Rock Engineering*. 1989;**22**(1):1-23
- [4] Dowding CH, Pierce CE. Use of time domain reflectometry to detect bridge scour and monitor pier movement. In: *Proceedings of the Symposium on Time Domain Reflectometry in Environmental, Infrastructure, and Mining Applications*; 7-9 September 1994. Evanston, Illinois: U.S. Bureau of Mines; 1994
- [5] Osasan KS, Afeni TB. Review of surface mine slope monitoring techniques. *Journal of Mining Science*. 2010;**46**(2):177-186
- [6] Su MB, Chen IH, Liao CH. Using TDR cables and GPS for landslide monitoring in high mountain area. *Journal of Geotechnical and Geoenvironmental Engineering, ASCE*. 2009;**135**(8):1113-1121
- [7] Yin Y, Wang H, Gao Y, Li X. Real-time monitoring and early warning of landslides at relocated Wushan Town, the Three Gorges Reservoir, China. *Landslides*. 2010;**7**(3):339-349
- [8] O'Connor KM, Dowding CH. *GeoMeasurements by Pulsing TDR Cables and Probes*. Florida: CRC Press, Boca Raton; 1999
- [9] Federico A, Popescu M, Elia G, Fidelibus C, Internò G, Murianni A. Prediction of time to slope failure: A general framework. *Environment and Earth Science*. 2012;**66**(1):245-256
- [10] Su MB, Chen YJ. Multiple reflection of metallic time domain reflectometry. *Experimental Techniques*. 1998;**22**(1): 26-29
- [11] Drusa M, Bulko R. Rock slide monitoring by using TDR inclinometers. *Civil and Environmental Engineering*. 2016;**12**(2):137-144
- [12] Su MB. Fracture monitoring within concrete structure by time domain reflectometry. *Engineering Fracture Mechanics*. 1990;**35**(1/2/3):313-320
- [13] Su MB, Chen YJ. MTDR monitoring systems for the integrity of infrastructures. *Journal of Intelligent Material Systems and Structures*. 1999;**10**(3):242-247
- [14] Kane WF, Beck TJ. Rapid slope monitoring. *Civil Engineering*. 1996;**66**(6):56
- [15] Su MB, Chen YJ. TDR monitoring for integrity of structural systems. *Journal of Infrastructure Systems*. 2000;**6**(2):67-72
- [16] Dowding CH, Dussud ML, Kane WF, O'Connor KM. Monitor deformation in rock and soil with TDR sensor cables. *Geotechnical Instrumentation News*. 2003;**21**(2):51-59
- [17] Lin YS, Chen IH, Ho SC, Chen JY, Su MB. Applying time domain reflectometry to quantification of slope deformation by shear failure in a landslide. *Environment and Earth Science*. 2019;**78**(5):123-133
- [18] Ho SC, Chen IH, Lin YS, Chen JY, Su MB. Slope deformation monitoring in the Jiufenershan landslide using

time domain reflectometry technology.  
*Landslides*. 2019;**16**:1141-1151

[19] Chu YM, Ho SC, Chen IH, Su MB. Applying TDR technology to the automatic monitoring of sliding surface and deformation amount in Lusan landslide area. In: Conference on Sustainable Development and Disaster Prevention in Civil Engineering; June 2019, Kaohsiung, Taiwan; 2019. pp. 635-640 (in Chinese)

[20] Ho SC, Chen IH, Lin YS, Chen JY, Su MB. Using time domain reflectometry for monitoring slope movement in the Jiufenershan landslide. In: 20th Southeast Asian Geotechnical Conference and 3rd AGSSEA Conference, Jakarta, Indonesia; 2018

[21] Chen IH, Lin YS, Ho SC, Chen JY, Su MB. Applying time domain reflectometry technology to measure slope deformation in landslides. In: the 8th Civil Engineering Conference in the Asian region (CECAR8), Tokyo, Japan; 2019. GS-6-2\_GS-3, No.2

[22] Shou K, Chen Y, Liu H. Hazard analysis of Li-shan landslide in Taiwan. *Geomorphology*. 2009;**103**(1):143-153

[23] Shou KJ, Wang CF. Analysis of the Chiufengershan landslide triggered by the 1999 Chi-Chi earthquake in Taiwan. *Engineering Geology*. 2003;**68**(3-4):237-250

[24] Chang KT, Huang HC. Three-dimensional analysis of a deep-seated landslide in Central Taiwan. *Environment and Earth Science*. 2015;**74**(2):1379-1390

[25] Lo CM, Feng ZY. Deformation characteristics of slate slopes associated with morphology and creep. *Engineering Geology*. 2014;**178**:132-154